Free Radical Research, April 2010; 44(4): 430–440

Protective role of *ortho*-substituted Mn(III) *N*-alkylpyridylporphyrins against the oxidative injury induced by *tert*-butylhydroperoxide

ANA S. FERNANDES[1,2], JORGE GASPAR[2], M. FÁTIMA CABRAL[1], JOSÉ RUEFF[2], MATILDE CASTRO[1], INES BATINIC-HABERLE[3], JUDITE COSTA[1] & NUNO G. OLIVEIRA[1,2]

[1]*iMed.UL, Faculty of Pharmacy, University of Lisbon, Lisboa, Portugal,* [2]*CIGMH, Department of Genetics, Faculty of Medical Sciences, New University of Lisbon, Lisboa, Portugal, and* [3]*Department of Radiation Oncology, Duke University Medical School, Durham, NC, USA*

(Received date: 30 October 2009; In revised form date: 9 December 2009)

Abstract

The present work addresses the role of two *ortho*-substituted Mn(III) *N*-alkylpyridylporphyrins, alkyl being ethyl in MnTE-2-PyP^{5+} and n-hexyl in MnTnHex-2-PyP^{5+}, on the protection against the oxidant *tert*-butylhydroperoxide (TBHP). Their protective role was studied in V79 cells using endpoints of cell viability (MTT and crystal violet assays), intracellular $O_2^{\bullet-}$ generation (dihydroethidium assay) and glutathione status (DTNB and monochlorobimane assays). MnPs *per se* did not show cytotoxicity (up to 25 μM, 24 h). The exposure to TBHP resulted in a significant decrease in cell viability and in an increase in the intracellular $O_2^{\bullet-}$ levels. Also, TBHP depleted total and reduced glutathione and increased GSSG. The two MnPs counteracted remarkably the effects of TBHP. Even at low concentrations, both MnPs were protective in terms of cell viability and abrogated the intracellular $O_2^{\bullet-}$ increase in a significant way. Also, they augmented markedly the total and reduced glutathione contents in TBHP-treated cells, highlighting the multiple mechanisms of protection of these SOD mimics, which at least in part may be ascribed to their electron-donating ability.

Keywords: *MnTE-2-PyP, MnTnHex-2-PyP, superoxide dismutase mimetic,* tert*-butylhydroperoxide, cytotoxicity, glutathione*

Abbreviations: *CV, crystal violet; DHE, dihydroethidium; DTNB, 5,5'-dithiobis(2-nitrobenzoic acid); γ-GCS, γ-glutamylcysteine synthetase; GSH, reduced glutathione; GSHt, total glutathione content (GSH+GSSG); GSSG, oxidized glutathione; GST, glutathione-S-transferase; mCB, monochlorobimane; MnPs, manganese (Mn) porphyrins; MnTE-2-PyP^{5+}, Mn(III) 5,10,15,20-tetrakis(N-ethylpyridinium-2-yl)porphyrin; MnTM-4-PyP^{5+}, Mn (III) 5,10,15,20-tetrakis(N-methylpyridinium-4-yl)porphyrin; MnTnHex-2-PyP^{5+}, Mn(III) 5,10,15,20-tetrakis(N-n-hexylpyridinium-2-yl)porphyrin; MTT, 3-(4,5-dimethylthiazol-2-yl)-2,5-diphenyl-2H-tetrazolium bromide; NHE, normal hydrogen electrode; PBS, phosphate buffered saline; ROS, reactive oxygen species; SOD, superoxide dismutase; SODm, superoxide dismutase mimetics; TBHP, tert-butylhydroperoxide; V79 cells, Chinese hamster cells.*

Introduction

The over-production of superoxide anion ($O_2^{\bullet-}$) is associated with inflammation and tissue injury, being thus related to a large number of pathophysiological conditions [1]. Superoxide dismutase (SOD) enzymes are metalloproteins that catalyse $O_2^{\bullet-}$ dismutation, detoxifying cells from superoxide [1–3]. The over-expression of SOD enzymes has been shown to have protective and beneficial roles, both in cell culture and in animal models of oxidative stress [4–7]. However, the use of native SOD as a therapeutic agent is

Correspondence: Nuno G. Oliveira, iMed.UL, Faculty of Pharmacy, University of Lisbon, Av. Prof. Gama Pinto 1649-003 Lisboa, Portugal. Tel: +351 217946400. Fax: +351 217946470. Email: ngoliveira@ff.ul.pt

ISSN 1071-5762 print/ISSN 1029-2470 online © 2010 Informa UK Ltd. (Informa Healthcare, Taylor & Francis AS)
DOI: 10.3109/10715760903555844

restricted by its low cell permeability, short circulating half-life, antigenicity and expense [8]. To overcome these limitations, low molecular-weight SOD mimetics (SODm) have been developed [8–15].

Manganese porphyrins (MnPs) are among the most effective functional catalytic antioxidants [9,16] and have been showing remarkable effects in different models of oxidative stress [17]. These compounds have the ability to scavenge a wide range of ROS, namely $O_2^{\bullet-}$, $ONOO^-$ and peroxyl radicals [17]. The SOD-like activity of the MnPs involves the alternate reduction and oxidation of the Mn centre, which results in changes in valence between Mn(III) and Mn(II), much like native SODs [10]. The ability of MnPs to scavenge $ONOO^-$ is related to the formation of an oxo–Mn(IV) complex that is reduced to Mn(III) by endogenous antioxidants [18]. The mechanism of lipid peroxidation inhibition by MnPs is thought to be analogous to that mentioned for $ONOO^-$ scavenging [8,17]. The mitigation of oxidative stress injury by MnPs seems to involve not only the direct scavenging of ROS/RNS, but also the modulation of redox-active transcription factors, such as HIF-1α, NF-κB and AP-1 [19–23].

Recently, we have reported cell-based studies to address the role of the Mn(III) *para* methylpyridylporphyrin, MnTM-4-PyP, on the protection against the cytotoxicity induced by three oxidants: xanthine/xanthine oxidase, *tert*-butylhydroperoxide (TBHP) and doxorubicin [24]. In this study, the possibility of evaluating *ortho*-substituted analogues was raised. *Ortho*-substituted porphyrins have been developed based on structure-activity relationship [10,11,16] and possess among the highest catalytic rate constants for $O_2^{\bullet-}$ dismutation, due to a combined effect of inductive, resonance, steric and electrostatic factors [10]. When the positive charge is moved from *para* onto *ortho* position of the pyridyl groups, i.e. closer to the porphyrin ring, the redox potential at the manganese site shifts to~+300 mV vs NHE. This is the midway potential between the oxidation and reduction of $O_2^{\bullet-}$ which allows equal facilitation for both steps of the dismutation process and thus the optimal k_{cat} on thermodynamic basis. All SOD enzymes, independently of the type of metal centre, dismute $O_2^{\bullet-}$ around that potential. Another factor that contributes to the antioxidant potency of the *ortho* isomers is the presence of positive charges close to the porphyrin ring that guide negatively charged $O_2^{\bullet-}$ to the metal centre [16,25,26]. It has been further demonstrated that k_{cat} for the $O_2^{\bullet-}$ dismutation parallels the rate constant for $ONOO^-$ reduction. Same thermodynamic as well as electrostatic facilitation for the approach of negatively-charged $ONOO^-$ to the Mn site is assured [18]. Finally, and as stated above, the same mechanism of action with peroxyl radical as with $ONOO^-$ is presumably operative. When compared to *para* analogues, the *ortho* isomers are further bulkier and thus do not interact significantly with nucleic acids, and are in turn expected to be less toxic [10]. The present work studies two *ortho*-substituted MnPs, MnTE-2-PyP and MnTnHex-2-PyP. These MnPs are nearly identical in terms of $O_2^{\bullet-}$ dismuting and $ONOO^-$ reducing abilities [16,18]. However, MnTnHex-2-PyP is 13 500-fold more lipophilic than MnTE-2-PyP and thus more prone to enter the cell [27,28]. *Ortho*-substituted MnPs have already shown remarkable protective effects in *in vitro* and *in vivo* models of oxidative stress injuries [9,19,23]. However, a thorough knowledge on the effects at the cellular level is still missing. In our previous work [24], MnTM-4-PyP was shown to be a potent antioxidant against the toxic effects of TBHP in V79 cells. In the present work we aim to evaluate the protection afforded by MnTE-2-PyP and MnTnHex-2-PyP against the same oxidative stress inducer. We also aimed to explore if enhanced lipophilicity of hexyl analogue makes it a more potent compound in this study. Recently, 6 Mn porphyrins, 3 Mn salens and 2 Mn cyclic polyamines in radioprotection of ataxia telangiectasia cells were compared, among them MnTE-2-PyP and MnTnHex-2-PyP [29]. While MnTnHex-2-PyP was efficacious, the equally potent antioxidant, but hydrophilic MnTE-2-PyP was not. The study indicated the critical role of compound bioavailability and suggested that the accumulation of hexyl analogue within mitochondria may be in the origin of its efficacy.

Tert-butylhydroperoxide is a short chain analogue of lipid hydroperoxides that has been often used as a model to investigate the mechanism of cell injury initiated by acute oxidative stress in a variety of cells [30–35]. Because of the higher stability and presence of the hydrophobic butyl moiety which allows easier membrane penetration, TBHP provides a convenient alternative to the natural oxidants hydrogen peroxide and lipid hydroperoxide [35]. TBHP penetrates cell membranes [35,36] and can generate free radical intermediates, namely alkoxyl and peroxyl radicals [33,37] and superoxide anion [24,36]. Cell injury can consequently occur by different phenomena, including changes in mitochondrial permeability [37], oxidative DNA damage, lipid peroxidation [38] and apoptosis [34]. Moreover, inside the cell, TBHP can be reduced to *t*-butanol by GSH peroxidase [35], promoting the depletion of intracellular GSH as reported in hepatocytes and other cell types [33,35,38–42]. Glutathione is the main non-enzymatic antioxidant defense within the cell; the GSH/GSSG ratio reflects the cellular redox state [30,43]. Since thiol homeostasis determines critical aspects of cell function and response [32], an imbalance at this level will further contribute to cell injury.

The present study aims to evaluate and compare the role of optimized MnPs, MnTE-2-PyP and MnTnHex-2-PyP against the TBHP-induced cell injury, using a multilevel approach. In order to achieve this

goal two complementary cell viability assays, the 3-(4,5-dimethylthiazol-2-yl)-2,5-diphenyl-2*H*-tetrazolium bromide (MTT) reduction and the crystal violet (CV) were used. ROS generation was assessed using the fluorescent probe dihydroethidium (DHE). The total glutathione (GSHt) and the oxidized glutathione (GSSG) contents were measured by the 5,5'-dithiobis(2-nitrobenzoic acid) (DTNB) assay. Also, the reduced glutathione, expressed as a percentage of the GSH content relative to non-treated control cells was assessed using the monochlorobimane (mCB) assay.

Materials and methods

Chemicals

Phosphate buffered saline (PBS; 0.01 M phosphate buffer, 0.138 M NaCl, 0.0027 M KCl, pH 7.4), Ham's F-10 medium, newborn calf serum, penicillin-streptomycin solution, trypsin, MTT, crystal violet, *tert*-butylhydroperoxide, 5-sulphosalicylic acid, glutathione reductase from baker's yeast, reduced glutathione, DTNB, nicotinamide adenine dinucleotide phosphate (NADPH) and glutathione-S-transferase (GST) from equine liver were obtained from Sigma-Aldrich (St. Louis, MO, USA). A stock solution of GST (10 U/mL) was prepared in PBS with 10% glycerol, aliquotized and stored at –18°C. Dimethylsulphoxide (DMSO) and ethanol were purchased from Merck (Darmstadt, Germany). Oxidized glutathione (GSSG) and monochlorobimane were obtained from Fluka (Buchs, Switzerland). A stock solution of mCB (10 mM) was prepared in ethanol, aliquotized and stored at −18°C. DHE was purchased from Molecular Probes (Eugene, OR, USA). A 10 mM stock solution of DHE was prepared in DMSO, aliquotized and stored under N_2, at −18°C. Mn porphyrins MnTE-2-PyP and MnTnHex-2-PyP (Figure 1) were synthesized as previously described [12].

Cell culture

V79 Chinese hamster cells (MZ), kindly provided by Professor H. R. Glatt (Germany), were routinely maintained in 175 cm^2 culture flasks (Sarstedt; Newton, NC, USA). Ham's F-10 medium supplemented with 10% newborn calf serum, 100 U/mL penicillin and 100 μg/mL streptomycin was used as the cell culture medium. The cells were kept at 37°C, under an atmosphere containing 5% CO_2.

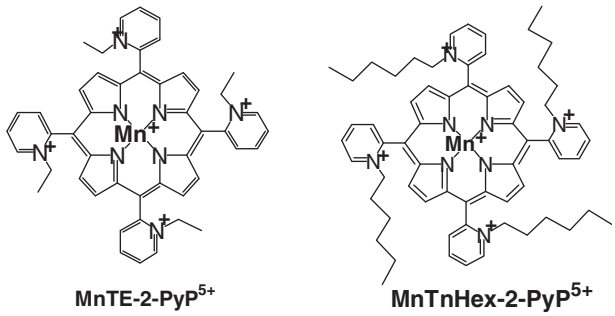

Figure 1. Chemical structures of the Mn(III) porphyrins MnTE-2-PyP and MnTnHex-2-PyP (Charges are omitted throughout text for clarity).

MTT reduction assay

The MTT reduction assay was performed according to previously described procedures [24,44]. Briefly, ~6 × 10^3 cells were cultured in 200 μL of culture medium per well in 96-well plates and incubated for 24 h at 37°C under a 5% CO_2 atmosphere. The culture medium was then replaced by fresh medium and cells were treated for 24 h with TBHP (100–300 μM) in the presence or absence of MnPs (0.1–25 μM). The cytotoxicity induced by the MnPs *per se* was evaluated under the same experimental conditions. After the treatments, the cells were washed with culture medium and MTT (0.5 mg/mL) was added to each well. The cells were grown for a further period of 2.5 h and then carefully washed with PBS. DMSO (200 μL) was added to each well and absorbance was read at 595 nm in a Zenyth 3100 microplate reader. Three-to-six independent experiments were performed and eight replicate cultures were used for each concentration in each independent experiment.

Crystal violet assay

The CV assay was performed as described in Fernandes et al. [24]. Approximately 3.5 × 10^3 cells were cultured in 200 μL of culture medium per well in 96-well plates and incubated at 37°C under a 5% CO_2 atmosphere. After 24 h, the culture medium was changed and cells were treated with TBHP (100 μM) with or without the MnPs (1–25 μM) for a 24-h period. The cells were then washed with PBS to remove non-adherent cells. The adherent cells were fixed with 96% ethanol for 10 min and then stained with 0.1% crystal violet in 10% ethanol for 5 min at room temperature. After staining, the extracellular dye was removed by rinsing thoroughly the cell monolayers with tap water. The remaining cell-attached dye was dissolved in 200 μL of 96% ethanol with 1% acetic acid and the absorbance was measured at 595 nm in a Zenyth 3100 microplate reader. Three-to-seven independent experiments were performed, each one comprising eight replicate cultures.

DHE fluorimetric assay

The DHE assay was performed as described in Fernandes et al. [24]. Approximately 2 × 10^4 cells/well were cultured for 24 h in 96-well plates (black-wall/clear-bottom; Costar 3603). Afterwards, the culture

medium was changed and cells were exposed for 3 h to TBHP (100 μM) in the presence or absence of the MnPs (5 μM). DHE was added at a final concentration of 10 μM. After the treatments, the cells were carefully washed with PBS; 200 μL of PBS were then added to each well and the fluorescence was determined in a Zenyth 3100 multimode detection microplate reader, using $\lambda_{excitation}=485$ nm and $\lambda_{emission}=595$ nm. The results were expressed as percentages of non-treated control cells, after subtracting the background fluorescence. Five independent experiments were performed, each comprising six replicate cultures for each experimental point.

DTNB assay

The DTNB assay [45,46] was used to quantify the GSHt and GSSG contents. V79 cells were cultured in Petri dishes (~ 3.0×10^4 cells/mL of culture medium) and incubated for 24 h at 37°C, under a 5% CO_2 atmosphere. The culture medium was then replaced by fresh medium and cells were treated for a further 24-h period with TBHP (100 μM) in the presence or absence of the MnPs (5 μM). After this incubation, cells were carefully washed, scrapped with ice-cold PBS and centrifuged for 10 min at 200 × *g*. The obtained pellet was suspended in PBS and submitted to two freeze-thaw cycles (−80°C/room temperature). An aliquot of this lysate was saved for the analysis of protein content by the Bradford assay and for the mCB assay. Sulphosalicylic acid was added to the remaining volume of lysate at a final concentration of 3% and this suspension was centrifuged for 10 min at 12 000 × *g*, 4°C. The obtained supernatant was divided for the quantification of the GSHt and GSSG. GSH and GSSG standard solutions were prepared in 3% sulphosalicylic acid. For the GSSG quantification, both samples and GSSG standards were treated with 2-vinylpyridine (2.5%) to derivatize GSH. The pH was adjusted to~6 with triethanolamine and the samples were incubated for 1 h at 4°C before the assay.

In a 96-well microplate, the GSHt and GSSG samples and standards were mixed with a freshly made solution containing glutathione reductase and DTNB, in phosphate buffer 0.1 M (pH 7.0, containing 1 mM EDTA). The reaction was started by the addition of NADPH. The final concentrations in the reaction mixture were 0.125 U/mL of glutathione reductase, 0.028 mg/mL of DTNB and 43 μM of NADPH. The kinetics of the absorbance increase at 405 nm was recorded at 4-min intervals over a 20-min period. The glutathione concentration in the samples was calculated by comparing the slopes of the sample with those of the correspondent standard curve and the result was expressed in nmol/mg protein. At least nine independent experiments were performed for the GSHt content and four were performed for the GSSG determination. Each independent experiment comprised the analysis of all samples and standards in duplicate.

mCB assay

The mCB assay was adapted from Kamencic et al. [47]. mCB is a probe that reacts with GSH generating the adduct mCB–GSH that can be detected by fluorimetry [47,48]. In a black 96-well microplate, PBS was added to 20 μL of the cell lysate, 1 U/mL GST and 100 μM mCB at a final volume of 100 μL. The reaction microplate was incubated for 30 min in the dark, at 37°C, 100 rpm. The GSH–mCB adduct was then measured in a Zenyth 3100 multimode detection microplate reader, using $\lambda_{excitation}=405$ nm and $\lambda_{emission}=465$ nm. The results were expressed as %GSH of non-treated control cells, after subtracting the background fluorescence and normalizing to the protein content. At least five independent experiments were performed, each comprising two duplicate measurements.

Stability of MnPs

The stability of MnPs under the experimental conditions described in the previous assays was evaluated by UV/Vis spectroscopy, using the supernatants of the cell cultures incubated for 24 h with MnPs (5 μM) and/or TBHP (100 μM). The supernatant of non-treated control cultures was used as reference to adjust the baseline. Two independent assays were performed. Both for MnTE-2-PyP and for MnTnHex-2-PyP, the UV/Vis spectra of the supernatant of cultures treated with each MnP alone were identical to those of cultures treated with 'MnP+TBHP'. Therefore, under these experimental conditions, MnPs remain stable and no oxidative degradation occurs.

Statistical analysis

The Kolmogorov-Smirnov test was used to assess the normality of continuous variables. For the variables with a normal distribution the homogeneity of the variances was evaluated using the Levene test and the differences in mean values of the results observed in cultures with different treatments were evaluated by the Student's *t*-test. For non-normal variables the Mann-Whitney test was used. All analyses were performed with the SPSS statistical package (version 15, SPSS Inc., Chicago, IL).

Results

We first evaluated the effects induced by MnTE-2-PyP and MnTnHex-2-PyP *per se* in V79 cells, at concentrations up to 25 μM. After a 24 h-incubation period, no cytotoxicity was observed for MnPs, either

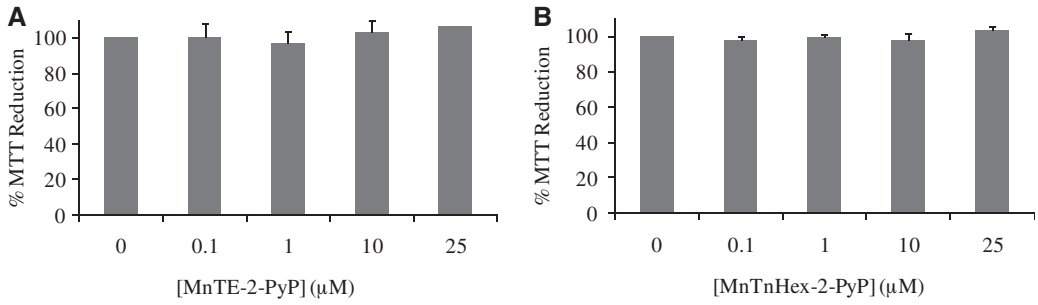

Figure 2. Cytotoxicity evaluation of MnTE-2-PyP (A) and MnTnHex-2-PyP (B). V79 cells were treated with the MnPs for 24 h and then submitted to the MTT assay.

using the MTT (Figure 2) or the CV assay (data not shown).

Figures 3 and 4 show the effect of MnTE-2-PyP against the cytotoxicity induced by TBHP. The exposure of V79 cells to TBHP (100 μM) resulted in a considerable decrease in the MTT reduction ($p < 0.01$), as well as in the CV staining ($p < 0.001$). The simultaneous treatment with MnTE-2-PyP led to a significant increase in the MTT reduction when compared with TBHP-treated cells, even for the 0.1 μM concentration (Figure 3A). At 5 μM, MnTE-2-PyP was highly protective, reverting the decrease in MTT reduction induced by TBHP ($p < 0.05$). The CV assay confirmed the significant protective effects of MnTE-2-PyP (1, 5 and 25 μM) against the TBHP-induced cytotoxicity (Figure 3B). To assess the effect of MnTE-2-PyP in more severe conditions, experiments using higher concentrations of TBHP were performed. As depicted in Figure 4, cultures treated for 24 h with 200 and 300 μM of TBHP showed a drastic cell death. The co-incubation with MnTE-2-PyP (1, 5 and 25 μM) showed significant protective effects ($p < 0.05$).

The effect of MnTnHex-2-PyP against the TBHP-induced cytotoxicity is shown in Figures 5 and 6. In the MTT assay (Figure 5A) this MnP also exerted a considerable protective effect, which was statistically significant ($p < 0.05$) for concentrations ≥ 1 μM. Like MnTE-2-PyP, 5 μM of MnTnHex-2-PyP was the lowest concentration that exhibited a maximum reversal of cell viability. The two MnPs have shown comparable cytoprotection profiles with both CV (Figures 3B and 5B) and MTT assays (Figures 3A, 4, 5A and 6). However, with MnTE-2-PyP the significant protective effects were seen at lower concentrations (0.1 μM). Furthermore, MnTE-2-PyP led to slightly higher cell viabilities in the CV assay, as well as in cultures treated with 200 μM of TBHP.

The data obtained in the DHE assay are depicted in Figure 7. The exposure of V79 cells to TBHP (100 μM, 3 h) led to a significant increase in the fluorescence intensity ($p < 0.01$). When cells were exposed to TBHP and MnTE-2-PyP or MnTnHex-2-PyP (5 μM), the fluorescence intensities returned to values lower than those presented by control cells ($p < 0.01$). The two MnPs showed a similar efficiency in reducing the intracellular ROS. It is also important to mention that cells treated only with the MnPs, either MnTE-2-PyP or MnTnHex-2-PyP, exhibited a considerable reduction in the hydroxyethidium fluorescence ($p < 0.01$), which could be ascribed to the abrogation of some level of oxidative stress that cells experience while growing in the medium or of the basal cellular ROS content.

The results of the glutathione status, as evaluated by the DTNB assay, are shown in Table I. V79 cells,

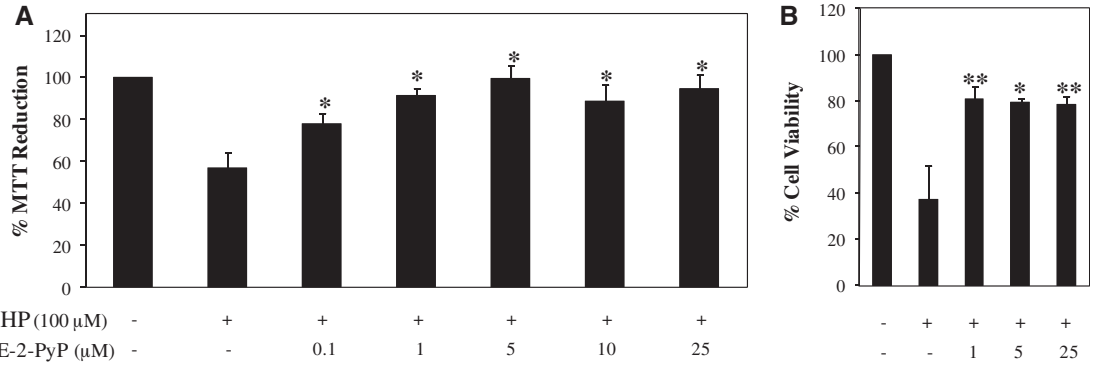

Figure 3. Effect of MnTE-2-PyP on the cytotoxicity induced by TBHP (100 μM) in V79 cells. Cells were incubated with increasing concentrations of MnTE-2-PyP in the presence of TBHP for 24 h and then submitted to the MTT (A) or to the CV staining (B) assays (*$p \leq 0.05$ and **$p \leq 0.01$, when compared with TBHP-treated cells in the absence of MnTE-2-PyP).

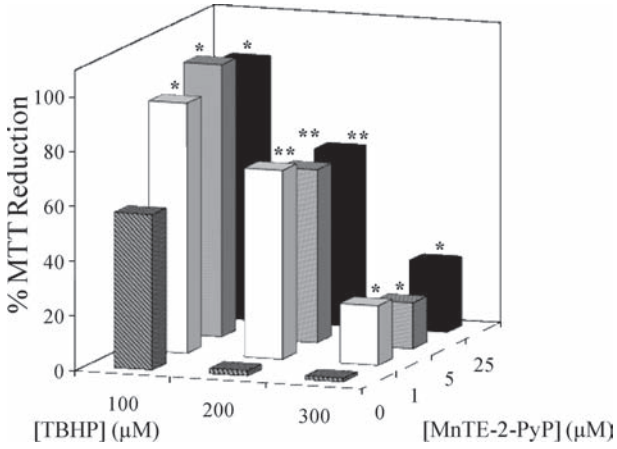

Figure 4. Effect of MnTE-2-PyP on the cytotoxicity induced by TBHP in V79 cells, as evaluated by the MTT assay. Cells were incubated with increasing concentrations of MnTE-2-PyP (1–25 μM) in the presence of different concentrations of TBHP (100–300 μM) for 24 h (*$p \leq 0.05$ and **$p < 0.01$, when compared with cells treated with the same concentration of TBHP in the absence of MnTE-2-PyP).

upon treatment with 100 μM TBHP, exhibited a marked depletion in the total glutathione content, that decreased from 7.69 to 2.50 nmol/mg prot ($p<0.001$). When cells were concomitantly exposed to TBHP and MnTE-2-PyP or MnTnHex-2-PyP, the GSHt increased to 16.54 and 19.71 nmol/mg prot, respectively. These increases were statistically significant ($p < 0.001$), when compared to the GSHt content of cells exposed only to TBHP. These cells also exhibited GSHt levels significantly above those of non-treated control cells ($p < 0.001$). The MnPs *per se* did not considerably change the GSHt content of V79 cells.

In control cells, as well as in cells treated only with MnTE-2-PyP or MnTnHex-2-PyP (5 μM), the levels of GSSG were low, having a small contribution for the total glutathione content. When V79 cells were treated with 100 μM TBHP, the GSSG level increased significantly ($p < 0.01$), accounting considerably for the GSHt observed in this case (Table I). Cells co-treated with TBHP and MnTE-2-PyP or MnTnHex-2-PyP, although having very high GSHt contents, did not show remarkable GSSG concentrations.

Besides the DTNB assay, a second approach to study the glutathione levels was followed—the mCB assay, that detects the reduced form of glutathione (GSH). The results obtained using this technique are depicted in Figure 8 and are expressed as a percentage of the GSH content of non-treated control cells, that presented an average fluorescence value of 3.1×10^4 RFU/μg prot. The treatment of V79 cells with the MnPs (5 μM) did not alter the GSH content. Cells treated with 100 μM TBHP showed a dramatic GSH depletion, having only ~22% of the GSH of control cells ($p < 0.001$). When cells were incubated simultaneously with TBHP and MnTE-2-PyP or MnTnHex-2-PyP, their GSH level increased markedly, not only restoring the depletion induced by TBHP ($p < 0.01$), but also reaching GSH values ~1.5-fold higher than those of control cells ($p < 0.001$).

Discussion

The implication of ROS, namely $O_2^{\bullet -}$, in numerous pathological phenomena supports the development of catalytic antioxidants. The most active SOD mimetics described so far are among the *ortho*-substituted MnPs [10,16,26,49]. However, a thorough knowledge on the effects at the cellular level is still lacking. In this context, we have studied the effects of two *ortho*-substituted MnPs, MnTE-2-PyP and MnTnHex-2-PyP, against the cytotoxic effects induced by TBHP. The studies were performed in V79 cells, a well-characterized fibroblast cell line widely used for cytotoxicity and cytogenetic studies.

Albeit TBHP is commonly used as an oxidant model, few studies to assess the effect of catalytic antioxidants towards this agent are available. The effects of the above-mentioned *ortho*-substituted MnPs were studied at three different levels: cytotoxicity, intracellular ROS level and glutathione status. Cytotoxicity was evaluated using a 24 h incubation

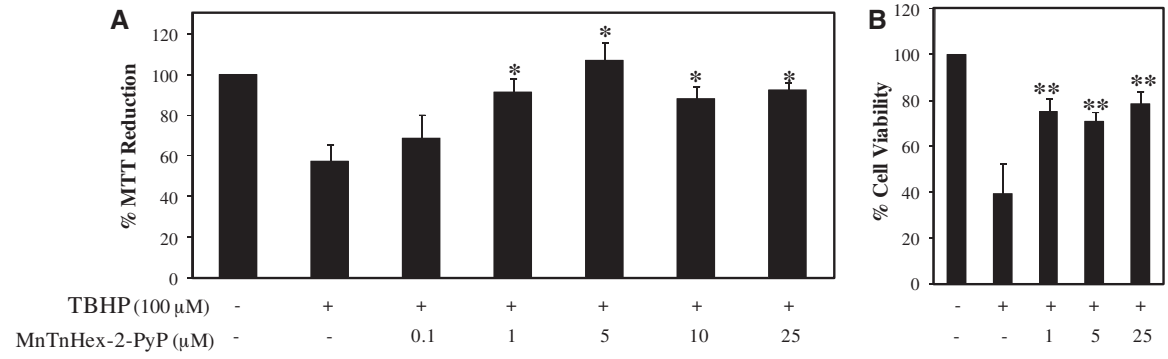

Figure 5. Effect of MnTnHex-2-PyP on the cytotoxicity induced by TBHP (100 μM) in V79 cells. Cells were incubated with increasing concentrations of MnTnHex-2-PyP in the presence of TBHP for 24 h and then submitted to the MTT (A) or to the CV staining (B) assays (*$p \leq 0.05$ and **$p \leq 0.01$, when compared with TBHP-treated cells in the absence of MnTnHex-2-PyP).

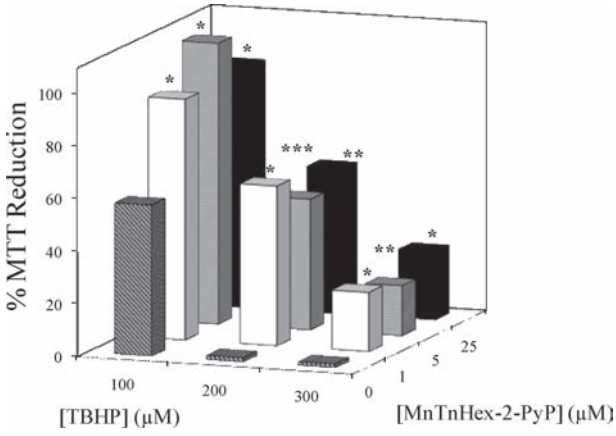

Figure 6. Effect of MnTnHex-2-PyP on the cytotoxicity induced by TBHP in V79 cells, as evaluated by the MTT assay. Cells were incubated with increasing concentrations of MnTnHex-2-PyP (1–25 μM) in the presence of different concentrations of TBHP (100–300 μM) for 24 h (*$p \leq 0.05$, **$p < 0.01$ and ***$p < 0.001$, when compared with cells treated with the same concentration of TBHP in the absence of MnTnHex-2-PyP).

period by the MTT assay and the CV staining method. Due to the limitations inherent to each method and since the assessment of an effect on cellular viability may depend on the assay chosen, the use of mechanistically different endpoints for cytotoxicity evaluation is usually recommended [50]. Therefore, we have primarily used the MTT assay, which is a measure of mitochondrial function [48,51] and, as a confirmatory assay, the CV method which is a colourimetric determination of adherent cells [24,50,52]. Using these assays, the MnPs *per se* did not show cytotoxicity up to 25 μM. Interestingly, with *Escherichia coli*, toxicity of MnTnHex-2-PyP was observed already at ≥3 μM levels [27,49].

Both MnPs have shown remarkable protective effects against the cytotoxicity induced by TBHP. The protection afforded by MnPs was lower in the CV assay than observed with the MTT assay, what may be attributed to the aforementioned mechanistic differences of the methods and also to the experimental protocols.

In a previous report [24], we have evaluated the performance of MnTM-4-PyP, a *para*-substituted MnP, in the same oxidative stress model. In the present work, both MnTE-2-PyP and MnTnHex-2-PyP were more effective than the *para*-analogue, showing better protectiveness at lower concentrations. This higher performance may be attributed to the greater antioxidant potency, since the *ortho* analogues have higher catalytic rate constants for $O_2^{\bullet-}$ dismutation and $ONOO^-$; reduction and, presumably, a higher rate constant for the reaction with peroxyl radicals than *para* isomers as well [53,54]. The reaction with peroxyl radical involves formation of $O=Mn^{IV}P$, which is also involved in the reaction with $ONOO^-$; the reactivity is related to the electron-deficiency of MnP that is similar with all *ortho* substituted alkylpyridylporphyrins; therefore the ability of MnPs to remove both $ONOO^-$ and peroxyl radical is likely similar also.

It has been reported that MnTE-2-PyP and MnTnHex-2-PyP possess identical antioxidant potency with respect to $O_2^{\bullet-}$, $ONOO^-$ and $CO_3^{\bullet-}$ [12,18]. Since MnTnHex-2-PyP is more prone to enter the cell due to its four orders of magnitude higher lipophilicity [27,28] one could expect this MnP to be more efficient than the ethyl analogue at lower doses. However, our results showed a slightly higher potency for MnTE-2-PyP. It has been reported that V79 cells have endocytic activity [55]. In view of this, it is possible that, despite the higher lipophilicity of MnTnHex-2-PyP, both MnPs have been uptaken by V79 cells in a similar way. It is also possible that the

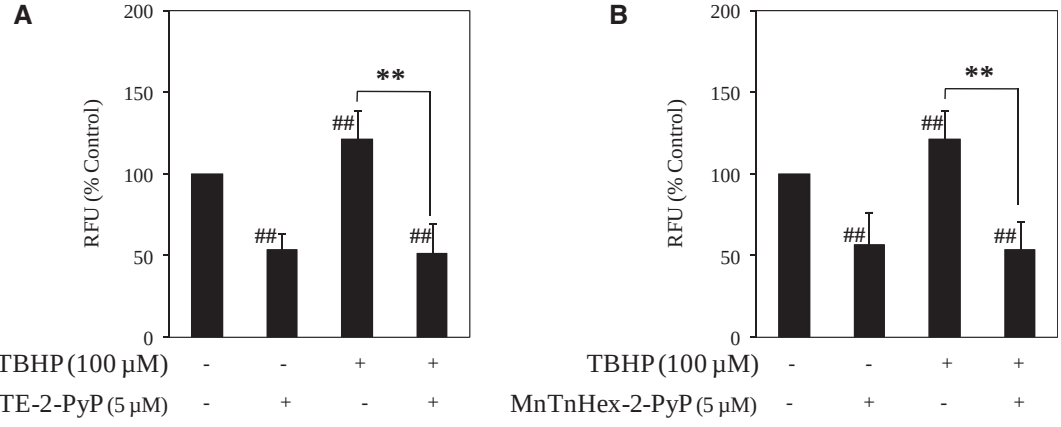

Figure 7. Effect of MnTE-2-PyP (A) and MnTnHex-2-PyP (B) on the DHE oxidation in V79 cells treated with TBHP (100 μM). Values (mean ± SD) represent relative fluorescence units (RFU), which approximately reflect the levels of superoxide anion, expressed as percentages of the control cells (##$p < 0.01$, when compared with non-treated control cells; **$p < 0.01$, when compared with cells treated with TBHP in the absence of MnP).

Table I. Effect of MnTE-2-PyP and MnTnHex-2-PyP on the changes in glutathione status induced by TBHP in V79 cells, as evaluated by the DTNB assay.

	Total GSH[a] (nmol/mg prot)	GSSG[b] (nmol/mg prot)
Non-treated control cells	7.69 ± 3.07	0.20 ± 0.10
MnTE-2-PyP 5 μM	8.20 ± 2.20	0.22 ± 0.19
MnTnHex-2-PyP 5 μM	7.34 ± 3.77	0.18 ± 0.11
TBHP 100 μM	2.50 ± 2.90$^{\#\#\#}$	1.07 ± 0.30$^{\#\#}$
TBHP 100 μM + MnTE-2-PyP 5 μM	16.54 ± 4.92$^{\#\#\#,***}$	0.46 ± 0.11$^{\#,*}$
TBHP 100 μM + MnTnHex-2-PyP 5 μM	19.71 ± 5.53$^{\#\#\#,***}$	1.58 ± 0.36$^{\#}$

[a]Values represent mean ± SD of at least nine independent experiments. [b]Values represent mean ± SD of four independent experiments. $^{\#}p < 0.05$, $^{\#\#}p < 0.01$ and $^{\#\#\#}p < 0.001$, when compared with non-treated control cells. $^{*}p < 0.05$ and $^{***}p < 0.001$, when compared with cells treated with TBHP alone.

protective effects occurred in extracellular millieu, plasma membrane and cytosolic space, rather than in mitochondria. As stated in the Introduction, were the effects expected on the mitochondrial level we would anticipate enhanced protectiveness of MnTnHex-2-PyP.

In this work we have also assessed the intracellular generation of superoxide anion, using the DHE assay. DHE is a cell permeable probe that reacts with $O_2^{\bullet-}$ to form the fluorescent product hydroxyethidium. Although its reaction with other ROS may interfere with the fluorescence peak, the oxidation of DHE is mostly superoxide dependent [56,57]. A 3-h incubation period was chosen due to the instability of ROS and also to avoid a pronounced cell death. Otherwise, changes in fluorescence intensity could result from differences in the number of cells and not necessarily in the level of ROS. Furthermore, the intracellular ROS production has been reported as an early event in TBHP-induced cytotoxicity [58]. In the present study TBHP led to a significant increase in the fluorescence intensity, indicating the intracellular production of $O_2^{\bullet-}$ by TBHP, which was abolished by both MnPs. This effect suggests that the scavenging of superoxide anion should be involved in the protection of the MnPs observed in the cytotoxicity assays. Along with the SOD-like activity, the ability of MnPs to decompose peroxyl radicals should also be a relevant mechanism for the abrogation of TBHP effects.

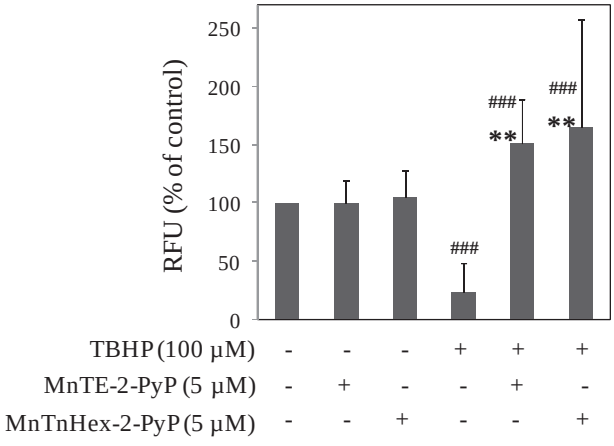

Figure 8. Effect of MnTE-2-PyP and MnTnHex-2-PyP (5 μM) on the glutathione depletion induced by TBHP (100 μM) in V79 cells, as evaluated by the mCB assay. Values (mean ± SD) represent relative fluorescence units (RFU) expressed as percentages of the control cells, after normalizing to the protein content of the lysate. Control cells exhibited an average fluorescence value of 3.1×10^4 RFU/μg prot ($^{\#\#\#}p < 0.001$, when compared with non-treated control cells; $^{**}p < 0.01$, when compared with cells treated with TBHP in the absence of MnP).

Glutathione is the main non-enzymatic antioxidant defense within the cell and its content, as well as the GSH/GSSG ratio, reflects the cellular redox state [35,43,59]. Under normal conditions, reduced GSH is largely predominant over GSSG, while with oxidative stress the percentage of GSSG can increase considerably [60]. To evaluate the glutathione status of cells submitted to different treatments, we have used two complementary approaches. The classical DTNB assay [45,46] was used to determine the total glutathione content and the GSSG concentration, and the fluorimetric mCB assay to assess the reduced form of glutathione.

Glutathione can reduce different hydroperoxides and radicals, and it has been reported to be depleted after an exposure to TBHP [32,33,40,42]. In addition, TBHP was previously shown to increase the GSSG level [30,61–63]. Our results concur with these previous reports either in terms of GSH depletion or GSSG increase.

The intracellular level of GSH is regulated by the γ-glutamylcysteine synthetase (γ-GCS) activity and by the availability of the precursor cysteine [64]. γ-GCS activity is rate limiting in the synthesis of GSH and this enzyme is subject to feedback regulation by the concentrations of glutathione [60]. Previous studies have shown that organic peroxides, and specifically TBHP, can stimulate the *de novo* biosynthesis of GSH [61,64], by up-regulating the expression of γ-GCS mRNA [63] and by increasing the activity of this enzyme [64]. In fact, Ochi [64] reported an increase in γ-GCS activity in V79 cells after a 1-h exposure to 100 μM TBHP. It is therefore expectable that TBHP is stimulating this enzyme under our experimental conditions. However, due to the ROS and lipid peroxides that TBHP generates and also due to the

glutathione peroxidase activity with this peroxide, the GSH formed is extensively consumed, oxidized to GSSG and extruded from cells [65–67], resulting in the depletion of GSHt and GSH and in the increase of GSSG. Conversely, in the presence of MnPs, an effective increase in the GSHt and GSH contents was observed. Along with the possible increase in γ-GCS-related activity, MnPs themselves seem to scavenge ROS, including lipid peroxides that are produced by TBHP insult, reducing the consumption of GSH. Our results provided herein add to other evidences that MnPs, due to their several *in vivo* easily accessible oxidation states (+2, +3, +4, +5), are both potent ROS/RNS scavengers, and powerful modulators of cellular redox-based metabolic pathways [19–21,23]. In addition, a MnP was previously shown to counteract the oxidative inactivation of isocitrate dehydrogenase [68], increasing the cellular supply of NADPH, which levels are known to be suppressed in TBHP-treated cells [69,70]. This may be also contributing to the increase in the GSH contents observed in cells treated with TBHP and MnPs.

In summary, this work shows that *ortho*-substituted MnPs are extremely potent antioxidants, with the ability to cope with the cellular damage induced by TBHP, even at low micromolar concentrations. Their clear protective effect in V79 cells was observed in terms of cytotoxicity and intracellular superoxide level. Also, for the first time, the results presented here reveal that these MnPs have an important role in enhancing reducing environment, which in turn favors reduced glutathione, thus assuring normal cellular redox status. Multiple mechanisms of cellular redox status protection by these antioxidants may be involved; the possible effect on the *de novo* GSH synthesis will be explored in our future studies.

Declaration of interest: A. S. F. acknowledges Fundação para a Ciência e a Tecnologia, Portugal, for financial support (PhD grant SFRH/BD/28773/2006). Ines Batinic-Haberle is thankful to Wallace H. Coulter Translational Partners Grant Program. The authors report no conflicts of interest. The authors alone are responsible for the content and writing of the paper.

References

[1] Halliwell B, Gutterdige JMC. Free radicals in biology and medicine. 4th ed. New York: Oxford University Press; 2007.

[2] Fridovich I. Superoxide ion radical, superoxide dismutases and related matters. J Biol Chem 1997;272:18515–18517.

[3] Fridovich I. Fundamental aspects of reactive oxygen species, or what's the matter with oxygen. Ann N Y Acad Sci 1999; 893:13–18.

[4] McCord J. Superoxide dismutase, lipid peroxidation and bell-shaped dose response curves. Dose Response 2008;6:223–238.

[5] Zhao Y, Xue Y, Oberley TD, Kiningham KK, Lin SM, Yen HC, Majima H, Hines J, St Clair D. Overexpression of manganese superoxide dismutase suppresses tumor formation by modulation of activator protein-1 signaling in a multistage skin carcinogenesis model. Cancer Res 2001;61:6082–6088.

[6] Zhao Y, Kiningham KK, Lin SM, St Clair DK. Overexpression of MnSOD protects murine fibrosarcoma cells (FSa-II) from apoptosis and promotes a differentiation program upon treatment with 5-azacytidine: involvement of MAPK and NFkappaB pathways. Antioxid Redox Signal 2001;3:375–386.

[7] Weydert CJ, Waugh TA, Ritchie JM, Iyer KS, Smith JL, Li L, Spitz DR, Oberley LW. Overexpression of manganese or copper-zinc superoxide dismutase inhibits breast cancer growth. Free Radic Biol Med 2006;41:226–237.

[8] Day BJ. Catalytic antioxidants: a radical approach to new therapeutics. Drug Discov Today 2004;9:557–566.

[9] Batinic-Haberle I, Reboucas JS, Spasojevic I. Superoxide dismutase mimics: their superoxide dismuting ability in aqueous solutions and protective effects in oxidative stress injuries *in vitro* and *in vivo*. Antiox Redox Signal 2009;under revision.

[10] Batinic-Haberle I, Benov L, Spasojevic I, Fridovich I. The *ortho* effect makes manganese(III) meso-tetrakis-(N-methylpyridinium-2-yl)porphyrin a powerful and potentially useful superoxide dismutase mimic. J Biol Chem 1998;273: 24521–24528.

[11] Batinic-Haberle I, Spasojevic I, Hambright P, Benov L, Crumbliss AL, Fridovich I. Relationship among redox potentials, proton dissociation constants of pyrrolic nitrogens, and *in vitro* and *in vivo* superoxide dismutating activities of manganese(III) and iron(III) water-soluble porphyrins. Inorg Chem 1999;38:4011–4022.

[12] Batinic-Haberle I, Spasojevic I, Stevens RD, Hambright P, Fridovich I. Manganese(III) *meso*-tetrakis(*ortho*-*N*-alkylpyridyl) porphyrins. Synthesis, characterization and catalysis of $O_2^{\cdot-}$ dismutation. J Chem Soc, Dalton Trans 2002;2689–2696.

[13] Riley DP, Henke SL, Lennon PJ, Weiss RH, Neumann WL, Rivers WJ Jr, Aston KW, Sample KR, Rahman H, Ling CS, Shieh JJ, Busch DH, Szulbinksi W. Synthesis, characterization, and stability of manganese(II) C-substituted 1,4,7,10,13-pentaazacyclopentadecane complexes exhibiting superoxide dismutase activity. Inorg Chem 1996; 35:5213–5231.

[14] Doctrow SR, Huffman K, Marcus CB, Tocco G, Malfroy E, Adinolfi CA, Kruk H, Baker K, Lazarowych N, Mascarenhas J, Malfroy B. Salen-manganese complexes as catalytic scavengers of hydrogen peroxide and cytoprotective agents: structure-activity relationship studies. J Med Chem 2002;45:4549–4558.

[15] Goldstein S, Samuni A, Merenyi G. Reactions of nitric oxide, peroxynitrite, and carbonate radicals with nitroxides and their corresponding oxoammonium cations. Chem Res Toxicol 2004;17:250–257. Erratum in: Chem Res Toxicol 2004;17: 1549.

[16] Rebouças JS, DeFreitas-Silva G, Spasojević I, Idemori YM, Benov L, Batinić-Haberle I. Impact of electrostatics in redox modulation of oxidative stress by Mn porphyrins: protection of SOD-deficient Escherichia coli via alternative mechanism where Mn porphyrin acts as a Mn carrier. Free Radic Biol Med 2008;45:201–210.

[17] Patel M, Day BJ. Metalloporphyrin class of therapeutic catalytic antioxidants. Trends Pharmacol Sci 1999;20:359–364.

[18] Ferrer-Sueta G, Vitturi D, Batinic-Haberle I, Fridovich I, Goldstein S, Czapski G, Radi R. Reactions of manganese porphyrins with peroxynitrite and carbonate radical anion. J Biol Chem 2003;278:27432–27438.

[19] Rabbani ZN, Spasojevic I, Zhang X, Moeller BJ, Haberle S, Vasquez-Vivar J, Dewhirst MW, Vujaskovic Z, Batinic-Haberle I. Antiangiogenic action of redox-modulating Mn(III) meso-tetrakis(N-ethylpyridinium-2-yl)porphyrin, MnTE-2-PyP^{5+}, via suppression of oxidative stress in a mouse model of breast tumor. Free Radic Biol Med 2009;47:992–1004.

[20] Zhao Y, Chaiswing L, Oberley TD, Batinić-Haberle I, St. Clair W, Epstein CJ, St. Clair D. A mechanism-based antioxidant approach for the reduction of skin carcinogenesis. Cancer Res 2005;65:1401–1405.

[21] Moeller BJ, Cao Y, Li CY, Dewhirst MW. Radiation activates HIF-1 to regulate vascular radiosensitivity in tumors: role of reoxygenation, free radicals and stress granules. Cancer Cell 2004;5:429–441.

[22] Tse HM, Milton MJ, Piganelli JD. Mechanistic analysis of the immunomodulatory effects of a catalytic antioxidant on antigen-presenting cells: Implication for their use in targeting oxidation/reduction reactions in innate immunity. Free Radic Biol Med 2004;36:233–247.

[23] Sheng H, Yang W, Fukuda S, Tse HM, Paschen W, Johnson K, Batinic-Haberle I, Crapo JD, Pearlstein RD, Piganelli J, Warner DS. Long-term neuroprotection from a potent redox-modulating metalloporphyrin in the rat. Free Radic Biol Med 2009;47:917–923.

[24] Fernandes AS, Serejo J, Gaspar J, Cabral MF, Bettencourt A, Rueff J, Castro M, Costa J, Oliveira NG. Oxidative injury in V79 Chinese hamster cells: protective role of the superoxide dismutase mimetic MnTM-4-PyP. Cell Biol Toxicol 2009, in press (doi: 10.1007/s10565-009-9120-3).

[25] Spasojevic I, Batinic-Haberle I, Reboucas JS, Idemori YM, Fridovich I. Electrostatic contribution in the catalysis of $O_2^{\cdot-}$-dismutation by superoxide dismutase mimics. MnIIITE-2-PyP^5+ versus MnIIIBr$_8$T-2-PyP+. J Biol Chem 2003;278: 6831–6837.

[26] Rebouças JS, Spasojevic I, Tjahjono DH, Richaud A, Méndez F, Benov L, Batinic-Haberle I. Redox modulation of oxidative stress by Mn porphyrin-based therapeutics: the effect of charge distribution. Dalton Trans 2008;1233–1242.

[27] Okado-Matsumoto A, Batinic-Haberle I, Fridovich I. Complementation of SOD-deficient *Escherichia coli* by manganese porphyrin mimics of superoxide dismutase activity. Free Radic Biol Med 2004;37:401–410.

[28] Kos I, Reboucas JS, DeFreitas-Silva G, Salvemini D, Vujaskovic Z, Dewhirst MW, Spasojevic I, Batinic-Haberle I. Lipophilicity of potent porphyrin-based antioxidants: comparison of ortho and meta isomers of Mn(III) *N*-alkylpyridylporphyrins. Free Radic Biol Med 2009;47:72–78.

[29] Pollard JM, Reboucas JS, Durazo A, Kos I, Fike F, Panni M, Gralla EB, Valentine JS, Batinic-Haberle I, Gatti RA. Radioprotective effects of manganese-containing superoxide dismutase mimics on ataxia telangiectasia cells. Free Radic Biol Med 2009;47:250–260.

[30] Nardini M, Pisu P, Gentili V, Natella F, Di Felice M, Piccolella E, Scaccini C. Effect of caffeic acid on *tert*-butyl hydroperoxide-induced oxidative stress in U937. Free Radic Biol Med 1998;25:1098–1105.

[31] Lee KJ, Choi CY, Chung YC, Kim YS, Ryu SY, Roh SH, Jeong HG. Protective effect of saponins derived from roots of *Platycodon grandiflorum* on *tert*-butyl hydroperoxide-induced oxidative hepatotoxicity. Toxicol Lett 2004;147:271–282.

[32] Macone A, Matarese RM, Gentili V, Antonucci A, Duprè S, Nardini M. Effect of aminoethylcysteine ketimine decarboxylated dimer, a natural sulfur compound present in human plasma, on tert-butyl hydroperoxide-induced oxidative stress in human monocytic U937 cells. Free Radic Res 2004;38:705–714.

[33] Alia M, Ramos S, Mateos R, Bravo L, Goya L. Response of the antioxidant defense system to *tert*-butyl hydroperoxide and hydrogen peroxide in a human hepatoma cell line (HepG2). J Biochem Mol Toxicol 2005;19:119–128.

[34] Kanupriya, Prasad D, Sai Ram M, Sawhney RC, Ilavazhagan G, Banerjee PK. Mechanism of tert-butylhydroperoxide induced cytotoxicity in U-937 macrophages by alteration of mitochondrial function and generation of ROS. Toxicol Vitro 2007;21:846–854.

[35] Volobоueva LA, Liu J, Suh JH, Ames BN, Miller SS. (R)-α-Lipoic acid protects retinal pigment epithelial cells from oxidative damage. Invest Ophthalmol Vis Sci 2005;46:4302–4310.

[36] Awe SO, Adeagbo ASO. Analysis of *tert*-butyl hydroperoxide induced constrictions of perfused vascular beds *in vitro*. Life Sci 2002;71:1255–1266.

[37] Piret J-P, Arnould T, Fuks B, Chatelain P, Remacle J, Michiels C. Mitochondria permeability transition-dependent *tert*-butylhydroperoxide-induced apoptosis in hepatoma HepG2 cells. Biochem Pharmacol 2004;67:611–620.

[38] Sohn JH, Han K-L, Lee S-H, Hwang J-K. Protective effects of panduratin A against oxidative damage of tert-butylhydroperoxide in human HepG2 cells. Biol Pharm Bull 2005;28:1083–1086.

[39] Chu C-Y, Tseng T-H, Hwang J-M, Chou F-P, Wang C-J. Protective effects of capillarisin on tert-butylhydroperoxide-induced oxidative damage in rat primary hepatocytes. Arch Toxicol 1999;73:263–268.

[40] Hwang J-M, Wang C-J, Chou F-P, Tseng T-H, Hsieh Y-S, Lin W-L, Chu C-Y. Inhibitory effect of berberine on tert-butyl hydroperoxide-induced oxidative damage in rat liver. Arch Toxicol 2002;76:664–670.

[41] Martín C, Martínez R, Navarro R, Ruiz-Sanz JI, Lacort M, Ruiz-Larrea MB. *tert*-Butyl hydroperoxide-induced lipid signaling in hepatocytes: involvement of glutathione and free radicals. Biochem Pharmacol 2001;62:705–712.

[42] Park JE, Yang J-H, Yoon SJ, Lee J-H, Yang ES, Park J-W. Lipid peroxidation-mediated cytotoxicity and DNA damage in U937 cells. Biochimie 2003;84:1198–1204.

[43] Schafer FQ, Buettner GR. Redox environment of the cell as viewed through the redox state of the glutathione disulfide/glutathione couple. Free Radic Biol Med 2001;30:1191–1212.

[44] Fernandes AS, Gaspar J, Cabral MF, Caneiras C, Guedes R, Rueff J, Castro M, Costa J, Oliveira NG. Macrocyclic copper(II) complexes: superoxide scavenging activity, structural studies and cytotoxicity evaluation. J Inorg Biochem 2007;101:849–858.

[45] Tietze F. Enzymic method for quantitative determination of nanogram amounts of total and oxidized glutathione: applications to mammalian blood and other tissues. Anal Biochem 1969;27:502–522.

[46] Anderson ME. Determination of glutathione and glutathione disulfide in biological samples. Methods Enzymol 1985;113: 548–555.

[47] Kamencic H, Lyon A, Paterson PG, Juurlink BHJ. Monochlorobimane fluorometric method to measure tissue glutathione. Anal Biochem 2000;286:35–37.

[48] Oliveira NG, Pingarilho M, Martins C, Fernandes AS, Vaz S, Martins V, Rueff J, Gaspar J. Cytotoxicity and chromosomal aberrations induced by acrylamide in V79 cells: role of glutathione modulators. Mutat Res 2009;676:87–92.

[49] Kos I, Benov L, Spasojević I, Rebouças JS, Batinic-Haberle I. High lipophilicity of meta Mn(III) N-alkylpyridylporphyrin-based SOD mimics compensates for their lower antioxidant potency and makes them equally effective as ortho analogues in protecting SOD-deficient E. coli. J Med Chem 2009;52:7868-7872.

[50] Chiba K, Kawakami K, Tohyama K. Simultaneous evaluation of cell viability by neutral red, MTT and crystal violet staining assays of the same cells. Toxicol Vitro 1998;12:251–258.

[51] Carmichael J, DeGraff WG, Gazdar AF, Minna JD, Mitchell JB. Evaluation of a tetrazolium-based semiautomated colorimetric assay: assessment of chemosensitivity testing. Cancer Res 1987;47:936–942.

[52] Mickuviene I, Kirveliene V, Juodka B. Experimental survey of non-clonogenic viability assays for adherent cells *in vitro*. Toxicol Vitro 2004;18:639–648.

[53] Bloodsworth A, O'Donnell VB, Batinic-Haberle I, Chumley PH, Day BJ, Crow JP, Freeman BA. Manganese-porphyrin reactions with lipids and lipoproteins. Free Radic Biol Med 2000;28:1017–1029.
[54] Day BJ, Batinic-Haberle I, Crapo JD. Metalloporphyrins are potent inhibitors of lipid peroxidation. Free Radic Biol Med 1999;26:730–736.
[55] Müller L, Kikuchi Y, Probst G, Schechtman L, Shimada H, Sofuni T, Tweats D. ICH-Harmonised guidances on genotoxicity testing of pharmaceuticals: evolution, reasoning and impact. Mutat Res 1999;436:195–225.
[56] Tarpey MM, Wink DA, Grisham MB. Methods for detection of reactive metabolites of oxygen and nitrogen: in vitro and in vivo considerations. Am J Physiol Regul Integr Comp Physiol 2004;286:R431–R444.
[57] Peshavariya HM, Dusting GJ, Selemidis S. Analysis of dihydroethidium fluorescence for the detection of intracellular and extracellular superoxide produced by NADPH oxidase. Free Radic Res 2007;41:699–712.
[58] Pias EK, Ekshyyan OY, Rhoads CA, Fuseler J, Harrison L, Aw TY. Differential effects of superoxide dismutase isoform expression on hydroperoxide-induced apoptosis in PC-12 cells. J Biol Chem 2003;278:13294–13301.
[59] Biswas SK, Rahman I. Environmental toxicity, redox signaling and lung inflammation: the role of glutathione. Mol Aspects Med 2009;30:60–76.
[60] Pastore A, Federici G, Bertini E, Piemonte F. Analysis of glutathione: implication in redox and detoxification. Clin Chim Acta 2003;333:19–39.
[61] Ochi T. Mechanism for the changes in levels of glutathione upon exposure of cultured mammalian cells to tertiary-butylhydroperoxide and diamide. Arch Toxicol 1993;67:401–410.

This paper was first published online on Early Online on 26 January 2010.

[62] Tormos C, Javier Chaves F, Garcia MJ, Garrido F, Jover R, O'Connor JE, Iradi A, Oltra A, Oliva MR, Sáez GT. Role of glutathione in the induction of apoptosis and c-fos and c-jun mRNAs by oxidative stress in tumor cells. Cancer Lett 2004;208:103–113.
[63] Kaur P, Kaur G, Bansal MP. Upregulation of AP1 by tertiary butyl hydroperoxide induced oxidative stress and subsequent effect on spermatogenesis in mice testis. Mol Cell Biochem 2008;308:177–181.
[64] Ochi T. Menadione causes increases in the level of glutathione and in the activity of γ-glutamylcysteine synthetase in cultured Chinese hamster V79 cells. Toxicology 1996;112:45–55.
[65] Eklow L, Moldeus P, Orrenius S. Oxidation of glutathione during hydroperoxide metabolism: a study using isolated hepatocytes and the glutathione reductase inhibitor 1,3-bis(2-chloroethyl)-l-nitrosourea. Eur J Biochem 1984;138:459–463.
[66] Ozaki M, Aoki S, Masuda Y. K^+-Linked release of oxidized glutathione induced by tert-butyl hydroperoxide in perfused rat liver is independent of lipid peroxidation and cell death. Jpn J Pharmacol 1994;65:183–191.
[67] Hayes JD, McLellan LI. Glutathione and glutathione-dependent enzymes represent a co-ordinately regulated defence against oxidative stress. Free Radic Res 1999;31:273–300.
[68] Batinic-Haberle I, Benov LT. An SOD mimic protects $NADP^+$-dependent isocitrate dehydrogenase against oxidative inactivation. Free Radic Res 2008;42:618–624.
[69] Pectu LG, Plaut GWE. NADP-specific isocitrate dehydrogenase in regulation of urea synthesis in rat hepatocytes. Biochem J 1980;190:581–592.
[70] Liu H, Kehrer JP. The reduction of glutathione disulfide produced by t-butyl hydroperoxide in respiring mitochondria. Free Radic Biol Med 1996;20:433–442.